Visualization of Atomic Processes on Ruthenium Dioxide using Scanning Tunneling Microscopy

H. Over,*[a] M. Knapp,[a] E. Lundgren,[b] A. P. Seitsonen,[c] M. Schmid,[d] and P. Varga[d]

The visualization of surface reactions on the atomic scale provides direct insight into the microscopic reaction steps taking place in a catalytic reaction at a (model) catalyst's surface. Employing the technique of scanning tunneling microscopy (STM), we investigated the CO oxidation reaction over the RuO_2(110) and RuO_2(100) surfaces. For both surfaces the protruding bridging O atoms are imaged in STM as bright features. The reaction mechanism is identical on both orientations of RuO_2. CO molecules adsorb on the undercoordinated surface Ru atoms from where they recombine with undercoordinated O atoms to form CO_2 at the oxide surface. In contrast to the RuO_2(110) surface, the RuO_2(100) surface stabilizes also a catalytically inactive c(2 × 2) surface phase onto which CO is not able to adsorb above 100 K. We argue that this inactive RuO_2(100)-c(2 × 2) phase may play an important role in the deactivation of RuO_2 catalysts in the electrochemical Cl_2 evolution and other heterogeneous reactions.

1. Introduction

Science and technology of catalysis is of central practical importance. About 80% of all technical chemicals are manufactured by utilizing heterogeneous catalysis.[1, 2] Heterogeneous catalysis is closely related to surface chemistry in that the reaction between the reactants takes place at the catalyst's surface.[2, 3] While present industrial catalysts are searched for by trial and error methods in combination with chemical intuition, a future challenge will be the design of atomically tailored catalysts with properties in activity and selectivity that are superior to conventional catalysts. The Au-Ni based catalyst for steam reforming[4a] and the bimetallic Co-Mo catalyst for ammonia synthesis[4b] are promising examples for such a design of catalysts. A necessary prerequisite for the atomic-scale design of catalyst is a detailed knowledge of the reaction mechanisms and the identification of elementary reaction steps in a catalyzed reaction. However, the processes on realistic catalysts are far too complex to allow for the identification of the microscopic reaction steps. This problem requires idealization of the experimental conditions. The so-called surface science approach[3] includes the use of single crystalline surfaces, serving as model catalysts, and investigations under well-controlled vacuum conditions (ultra high vacuum (UHV) conditions). While surface reactions on metal catalyst surfaces are quite well understood,[2,3] a deeper understanding of surface reactions on oxide surfaces is just emerging.[5–11]

The visualization of atomic processes at oxide surfaces using the technique of scanning tunneling microscopy (STM) is well appreciated.[11] The information provided by STM images is to some extent more direct (and therefore more appealing) than the information provided by alternative techniques such as low energy electron diffraction (LEED), thermal desorption spectroscopy (TPD), and vibrational spectroscopy. The strength of STM is the identification of defects on surfaces, either in the form of isolated adsorbates or isolated defects on the catalyst's surface. In general, the interpretation of STM images needs additional information such as provided by DFT (density functional theory) simulated STM images. The strength of this combined approach has been demonstrated, for instance, for the CO oxidation over RuO_2(110).[12, 13] Applying the technique of STM and other surface science techniques, the RuO_2 system has developed into a model system for metallic oxide surfaces.[14–16]

In the following we review the progress that has been made in the understanding of simple reactions on RuO_2 surfaces, applying the technique of STM. These results are compared with TiO_2, the model system in surface science of metal oxides.[11] All presented STM images are taken at room temperature (RT) and in the constant current mode. The assignment of particular features in STM images of RuO_2(110) is based on DFT calculations.[12]

[a] *Prof. H. Over, M. Knapp*
Department of Physical Chemistry, Justus-Liebig-University
Heinrich-Buff-Ring 58, 35392 Gießen (Germany)
Fax: (+49) 641-99-34559
E-mail: herbert.over@phys.chemie.uni-giessen.de

[b] *Dr. E. Lundgren*
Department of Synchrotron Radiation Research, University of Lund
Sölvegatan 14, 22362 Lund (Sweden)

[c] *Dr. A. P. Seitsonen*
Physikalisch Chemisches Institut, Universität Zürich
Winterthurerstraße 190, 8057 Zürich (Switzerland)

[d] *Prof. M. Schmid, Prof. P. Varga*
Institut für Allgemeine Physik, TU Wien
Wiedner Hauptstr. 8 – 10, 1040 Wien (Austria)

 DOI: 10.1002/cphc.200300833

2. STM Investigations of the Clean RuO_2(110) and RuO_2(100) Surfaces

2.1. Clean RuO_2(110) Surface

The RuO_2(110) surface can be produced by excessive exposure (typical 2×10^6 L O_2, 1 L = 1 Langmuir = 1.33×10^{-6} mbar s) of a well-prepared Ru(0001) surface to molecular oxygen, at a sample temperature of 650 K. The oxidation of Ru(0001) proceeds in an autocatalytic way,[17] a process first identified with the oxidation of ultra pure Pb.[18] Autocatalytic oxidation means that the Ru(0001) surface produces its own "catalyst" (that is, small RuO_2 nuclei) to accelerate the oxidation process.

In the bulk structure of RuO_2 (rutile structure) the Ru atoms bind to six oxygen atoms, forming a slightly distorted RuO_6 octahedron, while the O atoms are coordinated to three Ru atoms in a planar way that is consistent with an sp^2 hybridization of the O atom. The dimensions of the (110) surface unit cell are 3.12 Å × 6.38 Å. On the stoichiometric RuO_2(110) surface (see the ball-and-stick model of the bulk truncated RuO_2(110) surface: Figure 1 a) two kinds of undercoordinated surface atoms are present, namely the bridging oxygen atoms O_{br}, which are coordinated only to two Ru atoms underneath (instead of three) and the so-called 1 f-cus Ru atoms (1 f-cus stands for onefold coordinatively unsaturated sites).[19]

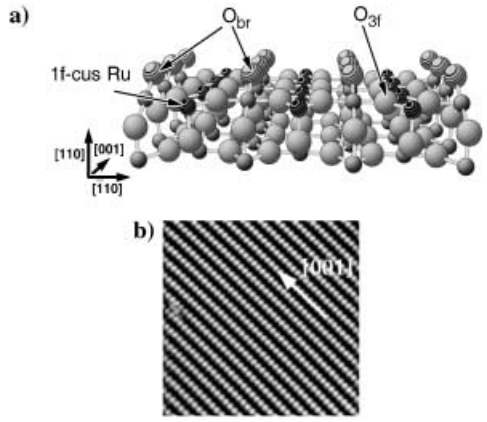

Figure 1. a) *Ball-and-stick model of the stoichiometric RuO_2(110) surface. Bulk O and Ru atoms are shown as large and small balls, respectively. A bridge-bonded O atom (O_{br}), a threefold coordinated lattice O atom (O_{3f}), and a onefold undercoordinated Ru atom (1 f-cus Ru) are indicated. b) Experimental STM image [constant current mode, taken at RT] of a stoichiometric RuO_2(110) surface: 20 nm × 20 nm, U = 0.95 V, I = 0.46 nA.*

The quality of the RuO_2(110) surface can be judged from the STM image in Figure 1 b. A well-ordered surface is imaged with long rows of protrusions and only one defect is discernable that is related to the dissociative adsorption of a single oxygen molecule (see section 3). If STM directly images the topography of the surface, the bright rows should be interpreted in terms of rows of bridging oxygen of RuO_2(110). However, for the structurally similar TiO_2(110) surface, the bridging O atoms have shown to be imaged in STM as depressions.[20] Note that STM topographies are always the result of both electronic and geometric effects. Therefore the interpretation of experimental STM images calls for DFT simulations. DFT simulations indicate that the bridging O atoms on RuO_2(110) are imaged as protrusions with an apparent corrugation of 0.3 Å across the bridging O rows.[12]

2.2. Clean RuO_2(100) Surface

The RuO_2(100) surface is prepared by excessive exposure of a well-prepared Ru(10$\bar{1}$0) surface to molecular oxygen (circa 3×10^5 L O_2), keeping the sample temperature at 700 K. The dimensions of the surface (1 × 1) unit cell are 3.12 Å × 4.28 Å. The LEED (low energy electron diffraction) pattern then exhibits a c(2 × 2) symmetry. CO adsorption experiments demonstrate that the c(2 × 2) LEED pattern consists actually of (1 × 1) domains in coexistence with c(2 × 2) domains.[21]

In Figure 2 we show a typical STM image of the RuO_2(100) surface together with a ball-and-stick model of the RuO_2(100)-(1 × 1) surface. The RuO_2(100)-(1 × 1) surface exposes bridging O atoms and 1 f-cus Ru atoms (see Figure 2 b) similar to the

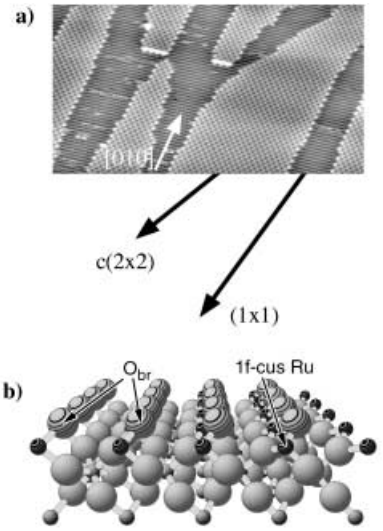

Figure 2. *a) Experimental STM image (constant current mode, taken at RT) of the RuO_2(100) surface: 12 nm × 30 nm, U = −0.80 V, I = 0.59nA. b) Ball-and-stick model of the stoichiometric RuO_2(100)-(1 × 1) surface. Bulk-O and Ru atoms are shown as large and small balls, respectively. A bridge-bonded O atom (O_{br}) and a onefold undercoordinated Ru atom (1 f-cus Ru) are indicated.*

RuO_2(110) surface. The main difference between both orientations is that on RuO_2(100) the bridging O atoms and the 1 f-cus Ru atoms are attached to each other, while on RuO_2(110) both undercoordinated surface species are well separated. We should mention that the surface structure of the RuO_2(100)-(1 × 1) surface has been resolved by quantitative LEED.[21] However, the surface structure of RuO_2(100)-c(2 × 2) is largely unknown. The existing data from the RuO_2(100)-c(2 × 2) structure point to a far reaching reconstruction of the RuO_2(100) surface.

The STM image in Figure 2 a documents nicely that there are two types of ordered phases on the RuO_2(100) surface, one with (1 × 1) symmetry and the other with c(2 × 2) symmetry. The bright spots on the (1 × 1) patches are assigned to bridging O

atoms. The (1×1) and $c(2 \times 2)$ patches form long stripes in the (010) direction. The $c(2 \times 2)$ domains are wider than the (1×1) domains. The widths of both domains are nearly constant across the surface, leading to an alternating sequence of $c(2 \times 2)$ and (1×1) domains. This pattern is reminiscent of modulated structures produced by the influence of mechanical stress, such as observed with the long-range spatial self-organization in the adsorbate-induced restructuring of the Cu(110)-(2×1)O surface.[22]

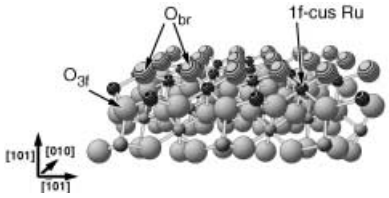

Figure 4. *Ball-and-stick model of the stoichiometric $RuO_2(101)$ surface. Bulk O and Ru atoms are shown as large and small balls, respectively. A bridge-bonded O (O_{br}) and a onefold undercoordinated Ru atom (1f-cus Ru) are indicated.*

2.3. Coexistence of Various Orientations of RuO_2

On the $Ru(10\bar{1}0)$ surface not only the (100) orientation of RuO_2 grows but also (to much lesser extent) the $RuO_2(110)$ and the $RuO_2(101)$ surfaces, as depicted in the next STM image (Figure 3). The much smaller total area of $RuO_2(110)$ and $RuO_2(101)$ is also

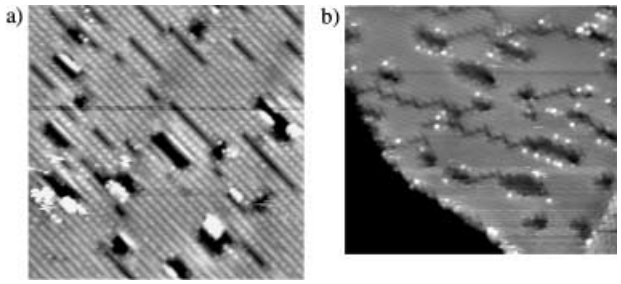

Figure 3. *Experimental STM image (constant current mode, taken at RT) of a) a $RuO_2(110)$ area on RuO_2 film grown on $Ru(10\bar{1}0)$: 20 nm $\times$ 20 nm, U = 0.0 V, I = 0.46 nA. b) A $RuO_2(101)$ area on RuO_2 film grown on $Ru(10\bar{1}0)$: 20 nm $\times$ 20 nm, U = $-$0.70 V, I = 0.53nA. The majority of the RuO_2 film grows in (100) orientation. The oxide film was treated by 3 L CO exposure and annealing to 525 K. This causes the formation of holes on the surface.*

consistent with the LEED pattern that does not indicate any diffraction spots from these orientations. The STM images were taken from a RuO_2 film that was produced at a temperature of 720 K so that the RuO_2 film on the $Ru(10\bar{1}0)$ is expected to be quite thick. This RuO_2 film was subsequently partly reduced by CO exposure at 525 K. Clearly, there are various regions on the surface with a symmetry that deviates from that of the $RuO_2(100)$ surface. A comparison with the images shown in section 2.1 demonstrates that RuO_2 grows also with (110) orientation on the $Ru(10\bar{1}0)$ surface (see Figure 3a) albeit with much smaller total area. The unit cell of the third type of RuO_2 domains (see Figure 3b) has dimensions of 4.5 Å $\times$ 5.5 Å which is close to that of the bulk truncated $RuO_2(101)$ surface (4.49 Å $\times$ 5.46 Å). We therefore assign this surface region to RuO_2 with (101) surface orientation. Again the total surface area of $RuO_2(101)$ on the RuO_2 film grown on $Ru(10\bar{1}0)$ is quite small compared to that with (100) orientation. Figure 4 shows a ball-and-stick model of the bulk truncated $RuO_2(101)$ surface, illustrating that this surface exposes also undercoordinated bridging O and 1f-cus Ru atoms such as $RuO_2(100)$ and $RuO_2(110)$. Therefore it is reasonable that all these orientations of RuO_2 reveal also similar catalytic activity in the oxidation of CO.[23]

The coexistence of various surface orientations in the growth of a RuO_2 film is also reconciled with our DFT calculations. The calculated surface energies of $RuO_2(110)$, $RuO_2(100)$ and $RuO_2(101)$ are similar: 71 meV Å^{-2} (110), 87 meV Å^{-2} (100) and 77 meV Å^{-2} (101).[16, 24] There is additional experimental evidence for the presence of multiple orientations of RuO_2. For instance, STM identified small regions of $RuO_2(100)$ for a 3 – 5 nm thick RuO_2 films grown on Ru(0001). Even thicker RuO_2 films on Ru(0001) become so rough that LEED does not exhibit a diffraction pattern.[25] Bulk RuO_2 crystals expose predominantly the (101) face[23] rather than (110). Last, in contrast to the gas preparation of RuO_2 films the electrochemical oxidation of Ru(0001) leads to a rough RuO_2 film oriented along the (100) direction.[26]

3. The Interaction of the $RuO_2(110)$ Surface with Oxygen from the Gas Phase

Oxygen exposure at room temperature populates a weakly bound oxygen species on the stoichiometric $RuO_2(110)$ surface. This oxygen species has been shown to reside in terminal position above the 1f-cus Ru atoms[27] and desorbs already at about 450 K.[28] The adsorption energy of the on-top O species is more than 1 eV lower than that of the bridging O atoms.[27, 29] In Figure 5a we show an STM image of the $RuO_2(110)$ surface that is

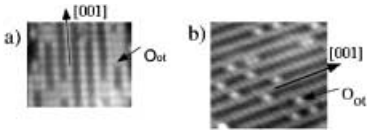

Figure 5. *a) 5 nm $\times$ 4 nm STM image (constant current mode, RT) of a $RuO_2(110)$ surface which was exposed to 0.1 L oxygen at room temperature (U = 0.01 V, I = 0.46 nA).[13] b) 6 nm $\times$ 6 nm STM image (constant current mode, RT) of a $RuO_2(110)$ surface which was exposed to 0.01 L oxygen at 350 K (U = $-$0.25 V, I = 1.83 nA).*

partly covered with the weakly bound oxygen species. Clearly additional bright features appear between the rows of bridging O atoms when compared to the stoichiometric surface (see Figure 1b).[12, 13] From the registry of these new features with respect to the bridging O atoms, the weakly bound oxygen atoms are inferred to adsorb on-top of the 1f-cus Ru atoms in agreement with a recently published LEED/DFT analysis.[27] Consecutive STM images of the same region disclose that the

mobility of the on-top O is negligibly small even at room temperature.

Another important aspect drawn from this STM image is that the additional protrusions appear always in pairs or multiples of pairs when dosing oxygen at room temperature. This observation supports the view that oxygen dissociation proceeds via a molecular oxygen precursor on the surface (see Figure 6). At temperatures below 100 K, molecular oxygen has been shown to

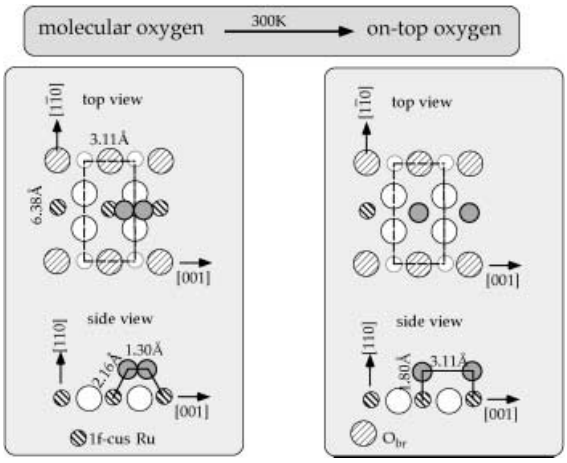

Figure 6. *Schematic view of the dissociative adsorption of molecular oxygen from the gas phase. First, at low temperatures (about 100 K) oxygen adsorbs molecularly (left side); the indicated bond lengths are determined by DFT calculations.[27] The oxygen molecules bridge two neighboring 1f-cus Ru atoms. When the surface is annealed to 300 K, the adsorbed oxygen molecule dissociates in two on-top oxygen atoms above the 1f-cus Ru atoms (right side).*

lie down on the RuO_2(110) surface (as an intact entity), bridging adjacent 1f-cus Ru atoms.[27] Increasing the sample temperature, some of the molecular oxygen desorbs, while the rest dissociates, making strong O–Ru bonds to the attached 1f-cus Ru atoms. Since the diffusion barrier of the on-top O species along the (001) direction is as high as 1.2 eV (according to DFT calculations[13, 15]), even at room temperature the on-top oxygen atoms are immobile. Henceforth, the distribution of on-top O atoms seen in room temperature STM represents the frozen-in configuration after the dissociation of adsorbed oxygen molecules. In contrast, oxygen exposure at 350 K leads to isolated on-top O species on the RuO_2(110) surface, as illustrated in Figure 5b. This means that at 350 K the on-top O species is mobile enough to diffuse on the RuO_2(110) surface although still some of the oxygen atoms are paired.

Recently, isotope labeling experiments give evidence of the exchange of on-top and bridging O atoms on the RuO_2(110) surface during the desorption of on-top oxygen.[30, 31]

4. The Mild Reduction of RuO_2 with CO

4.1. CO Oxidation over RuO_2(110)

Previous studies [TPD, HREELS (high resolution electron energy loss spectroscopy), STM, DFT][13, 32–35] have demonstrated that CO exposure to RuO_2(110) at room temperature results in a mild reduction of the surface in that the bridging O atoms are removed (and partly replaced by CO). The rest of the RuO_2(110) film is not affected by this reduction process. From DFT calculations[15, 34, 35] we know even more about the actual mechanism of the CO oxidation over RuO_2(110). CO adsorbs first molecularly above the 1f-cus Ru atoms (see Figure 7a),[36] and subsequently it forms the transition state (see Figure 7b)

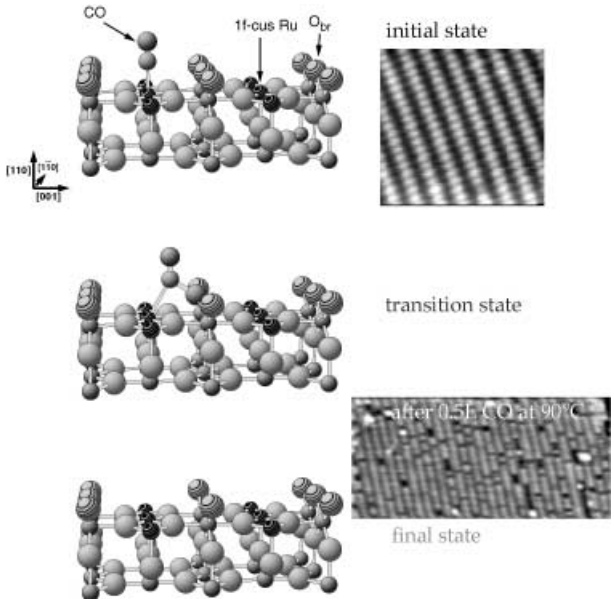

Figure 7. *a) The initial state for CO oxidation on RuO_2(110) is characterized by the adsorption of CO molecules on top of the 1f-cus Ru atoms. On the left side, the 5 nm × 4 nm STM image (constant current mode, RT) is taken from a clean RuO_2(110) surface.[13] The rows of bright protrusions are assigned to bridging O atoms. b) In the transition state both CO and the active oxygen (bridging O) atoms are drawn to each other (DFT calculations[16, 34]). c) The final state of the RuO_2(110) surface is characterized by vacancies in the rows of bridging O atoms due to the recombination of CO with bridging O atoms and the rapid release of the product CO_2 into the gas phase. The final state situation is shown in the left STM image.[13] The depressions (either isolated or in the form of small stripes) in the row of bridging O atoms are vacancies caused by the reaction with CO. The isolated bright spots in such vacancies are adsorbed CO molecules.*

where both CO and bridging O are drawn to one another. Finally, CO and bridging O recombine to form CO_2 that rapidly leaves the surface at room temperature. The final state of the catalyst's surface after this elementary reaction step is characterized by a bridging O vacancy (see Figure 7c). The final state situation was also imaged by STM (see Figure 7c right side[13]). The bright rows in Figure 7c are assigned to bridging O atoms on the RuO_2(110) surface. Occasionally we observe dark spots and short dark stripes in those rows which are ascribed to missing bridging O atoms. Illustrative DFT based movies of the CO oxidation reaction on RuO_2(110) can be found on the website given in ref. [37].

When exposing the RuO_2(110) surface to large amounts of CO (say 10 L CO at room temperature), all bridging O atoms are replaced by CO.[38] The corresponding STM image is shown in Figure 8a.[39] The bright spots are interpreted as CO molecules sitting above the 1f-cus Ru atoms. The faint grey rows (showing

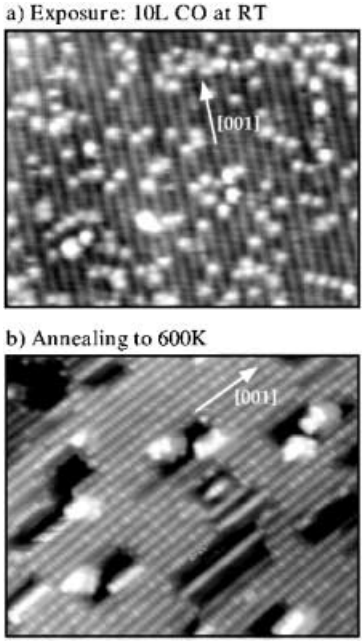

Figure 8. a) STM image (20 nm × 16 nm, U = − 1.08 V, I = 0.46 nA) of the RuO_2(110) surface after exposure of 10 L CO at room temperature.[39] Under these conditions the RuO_2(110) surface is mildly reduced in that all bridging O atoms are removed from the surface and replaced by bridging CO molecules. The bright protrusions with apparent height of 0.6 Å are CO molecules, sitting in on-top positions above the 1f-cus Ru atoms. b) STM image (20 nm × 16 nm, U = − 0.82 V, I = 3.34 nA) of the mildly reduced RuO_2(110) surface after annealing to 600 K. The removal of CO molecules is accompanied by the creation of 3.0 Å deep holes.[39]

an apparent corrugation across the rows of only 0.05 Å) in the STM image are assigned to the bridging CO molecules that had replaced the bridging O atoms.

Under reaction conditions, where CO and O_2 are exposed to the catalyst surface, two potentially active O species are present on the RuO_2(110) surface, namely the bridging O and the on-top O species. The adsorption energy of the on-top O atoms is lower (by more than 1 eV) than that of the bridging O atoms.[27] According to the Brønsted – Evans – Polanyi relation[40] the activation energy and the energy exchange of a given reaction are often related, that is, the greater the thermodynamic driving force for a reaction the lower its barrier will be. This relationship has recently been verified by DFT calculations for a couple of reactions.[41, 42] Therefore the on-top O species on RuO_2(110) is anticipated to be much more active in oxidizing CO than the bridging O atoms. This simple view, although it was apparently supported by recent high resolution electron energy loss Spectroscopy (HREELS) experiments,[34] has been challenged by recent isotope labeling experiments.[30]

4.2. CO Oxidation on RuO_2(100)

The mild reduction of the RuO_2(100)-(1 × 1) surface by CO exposure at room temperature is almost as efficient as of RuO_2(110). However, the (1 × 1) and the c(2 × 2) phases on the RuO_2(100) surface behave differently on CO exposure. The STM image in Figure 9a reveals that the CO exposure modifies the

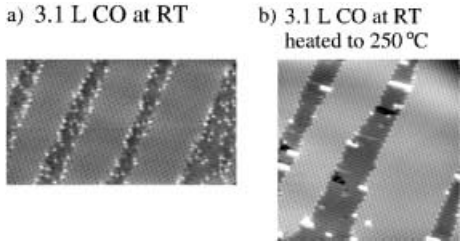

Figure 9. a) STM image (14 nm × 30 nm, U = − 0.14 V, I = 0.46 nA) of the RuO_2(100) surface after exposure of 3.1 L CO at RT. Under these conditions the RuO_2(100)-(1 × 1) surface is mildly reduced in that all bridging O atoms are replaced by CO molecules. The bright protrusions with an apparent height of 0.6 Å are CO molecules. The RuO_2(100)-c(2 × 2) phase is not influenced by the CO exposure. b) STM image (20 nm × 20 nm, U = 0.20 V, I = 0.40 nA) of the RuO_2(100) surface after exposure of 3.1 L CO at RT and annealing at 250 °C. Again, only the RuO_2(100)-(1 × 1) surface is affected by this treatment in that small pits are formed which are decorated by small protrusions interpreted as islands of metallic Ru.

(1 × 1) phase but leaves the c(2 × 2) patches untouched. With STM we see bright spots on the RuO_2(100)-(1 × 1) patches. These are ascribed to adsorbed CO molecules on the (1 × 1) phase after a sufficient number of bridging O atoms has been removed through reduction by CO.

This observation is consistent with previous LEED measurements.[21] The LEED intensities of particular c(2 × 2) and (1 × 1) spots during dosing CO indicate that CO readily adsorbs on RuO_2(100)-(1 × 1), while CO does not adsorb at all (even at a sample temperature as low as 100 K) on the RuO_2(100)-c(2 × 2) surface. Reactivity measurements give evidence that the RuO_2(100)-(1 × 1) surface is as active as the RuO_2(110) surface in oxidizing CO[23] and that the c(2 × 2) is inactive in oxidizing CO.[21] If the Ru(10$\bar{1}$0) surface is exposed to 6×10^5 L of O_2 at 875 K, the resulting RuO_2 film consists exclusively of RuO_2(100)-c(2 × 2).[43] This c(2 × 2) surface is not able at all to convert CO into CO_2. We argue that this inactive RuO_2(100)-c(2 × 2) phase may play an important role in the deactivation of RuO_2 catalysts in the electrochemical Cl_2 evolution.[44]

After annealing the mildly reduced RuO_2(100) surface to 530 K (see Figure 9b), the bright spots in STM disappear on the (1 × 1) and instead long bright und dark stripes appear on the (1 × 1) surface. The dark elongated stripes are interpreted in analogy to the RuO_2(110) surface as holes where part of the topmost double layer is missing (see discussion in section 4.3). The bright areas are assigned to metallic Ru islands. This assignment is justified by a comparison with the reduction behavior of RuO_2(110)[12, 39] (see discussion in section 4.3).

4.3. Restoration of a Mildly Reduced RuO_2(110) Surface

When heating the mildly reduced RuO_2(110) surface of Figure 8a to 600 K, the surface morphology changes drastically as seen in Figure 8b. The CO molecules in Figure 8a have disappeared in agreement with corresponding CO thermal desorption experiments.[35] However, small holes have been generated with an apparent depth of 3.0 Å. The corrugation across the bright rows is now again 0.3 Å and therefore much stronger than before the

annealing to 600 K (see section 4.1.) and similar to the stoichiometric RuO_2(110) surface (see section 2.1.). This observation may imply the reappearance of bridging O atoms on the surface, a conclusion which is corroborated by recent activity measurements on RuO_2(110).[35] It was demonstrated that the complete (mild) reduction of RuO_2(110) leads to an inactive surface which is no longer able to oxidize CO to CO_2 at room temperature due to the absence of bridging O atoms (that is, the active oxygen species) on the surface. However, upon anneal to temperatures above 500 K the activity of RuO_2(110) is at least partly restored. This effect was attributed to the reappearance of bridging O atoms on the RuO_2(110) surface.[35]

With this additional information in mind, we are able to explain the transformation of the RuO_2(110) surface shown in Figure 8a and Figure 8b. The mildly reduced RuO_2(110) surface is characterized by a surface where all bridging O atoms are replaced by CO without invoking further modifications of the surface. Annealing this surface to 600 K results in the desorption of the CO molecules on the oxide surface and the appearance of holes in the STM image. These holes are produced by the migration of 3-fold coordinated lattice O atoms to the bridge position, thereby populating the surface with active bridging oxygen atoms. The coordination of the Ru surface atoms attached to the released 3f-O atoms becomes too small. Therefore these undercoordinated Ru atoms are unstable and agglomerate to small metal islands at the rims of the holes. In the STM image these clusters are protruding by about 2 Å (see Figure 8b).[12] The Ru agglomeration in turn liberates further oxygen atoms which are used to cap 2f-cus Ru atoms by bridging O atoms. The complex processes occurring during a 600 K anneal of a mildly reduced RuO_2(110) surface are summarized in Figure 10. The mildly reduced RuO_2(100) surface separates after annealing into a restored oxide with holes and small Ru islands.

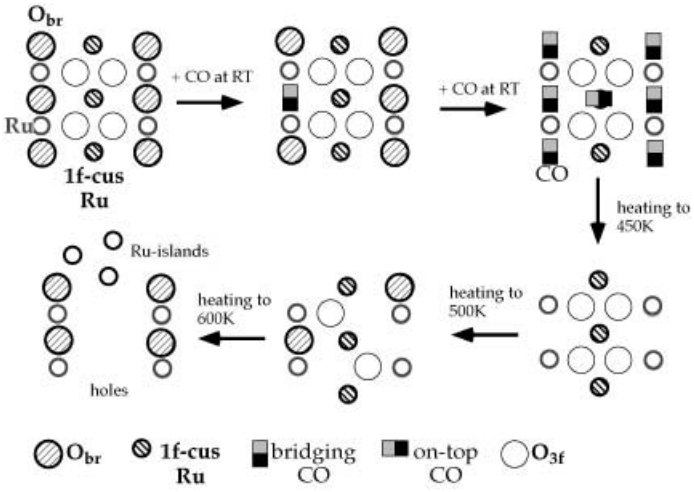

Figure 10. *A schematic summarizes the elementary steps in the reduction of the RuO_2(110) surface. First, CO molecules react with bridging O atoms and reside partly in the vacancies produced. With prolonged CO exposure, all bridging O atoms are replaced by asymmetric bridging CO molecules and partly also the 1f-cus Ru atoms are occupied by CO molecules. In STM, the latter CO species are imaged as 0.6 Å high protrusions (see Figure 9a). Upon heating the sample to 450 K, CO molecules desorb from the surface leaving a reduced RuO_2(110) surface with high surface energy (> 120 meV Å^{-2}). Annealing to 500 K results in a restructuring of the RuO_2(110) surface in that threefold coordinated surface oxygen transforms to bridging O atoms, thereby creating holes. The attached Ru atoms become too undercoordinated so that they agglomerate in small islands at the rims of the holes. With this process further surface oxygen is released and fills in the bridging O sites. In summary, we get an autocompensated RuO_2(110) surface with small Ru islands.*

5. Comparison with TiO_2(110)

Rutile TiO_2 is the model system in surface science of metal oxides that has recently been reviewed by Diebold.[11] Therefore a comparison of RuO_2 with TiO_2 may help to advance our understanding of metal oxide surfaces.

While RuO_2(110) and TiO_2(110) do reveal many physical properties in common, there are distinct differences as well. The rutile phases of TiO_2 and RuO_2 have similar lattice parameters. RuO_2 is however a metallic oxide with a high electronic conductivity, whereas rutile-TiO_2 is semiconducting, exhibiting a band gap of about 3 eV.[5] This difference in the electronic structure is also manifested in STM. For RuO_2(110) both polarities provides stable STM conditions. TiO_2(110) samples are in general n-type semiconducting. Therefore, only tunneling into unoccupied states of TiO_2(110) permits stable STM images.[45]

For the case of RuO_2(110) the STM is able to image the on-top oxygen. On TiO_2(110), the on-top species has not been identified with room temperature STM. Only recently, with a variable temperature STM Schaub et al.[46] were able to image on-top O atoms. In addition these authors unraveled an molecular oxygen-mediated diffusion mechanism of bridging O vacancies on rutile TiO_2(110).

The actual surface structure of TiO_2(110) is very sensitive to the reduction state of bulk TiO_2 as outlined by Diebold and co-workers.[47] In particular complex (1×2) reconstructions and a rosette-like structure have been identified.[48] But also the oxidation conditions and the history of the TiO_2(110) sample have a significant influence on the actual surface structure and morphology of the surface.[48] So far all STM experiments of RuO_2 have been performed on the ultrathin films that form on Ru upon oxidation. However, the interaction with the bulk may be equally important for RuO_2 as for TiO_2 and should therefore be investigated in the future.

The precise surface structure of TiO_2(110) is still a matter of debate as theory[49] and experiments[50] do not agree on the amplitude of the inward relaxation of the bridging O row. Quite in contrast, LEED and DFT derived surface structures of RuO_2(110) are virtually identical.[12]

The structure of catalytically inactive RuO_2(100)-c(2×2) is unknown. It is possible that this surface structure is related to the (3×1) reconstruction of TiO_2(100).[11, 51, 52]

From an STM point of view the major difference of RuO_2(110) and TiO_2(110) is the imaging of the bridging O atoms. While on TiO_2(110) the bridging O atoms are imaged as depressions,[20] on RuO_2(110) these atoms are imaged in bright contrast.[13] Accordingly, missing bridging O atoms are imaged as bright features on TiO_2(110) and as depressions on RuO_2(110). For the case of

TiO_2(110) this behavior was traced back to a purely electronic effect.[20] The charge density around the Fermi level was shown to be higher above the Ti atoms than above the O atoms.

The activity of TiO_2(110) and many other oxides is closely related to presence of defects on the surface.[53, 54] Quite in contrast, RuO_2(110) is active through the regular undercoordinated surface sites.[23, 55]

6. Conclusions

Hydrated RuO_2 has shown to be an efficient and robust catalyst for the CO oxidation at room temperature even by humid air.[56] Also on supported RuO_2 catalysts the CO oxidation has shown to be efficient.[57] Here, we reviewed STM measurements of the CO oxidation reaction on two different orientations of RuO_2. The bright features seen in atomically resolved STM images of the clean surfaces of RuO_2(110) and RuO_2(100) are assigned to bridging O atoms. The mild reduction of both RuO_2 surfaces at room temperature via CO exposure was studied by STM. The reaction mechanisms on both surfaces are practically identical in that CO first adsorbs over the undercoordinated Ru atoms (1f-cus Ru) from where the CO molecule recombines with adjacent bridging O atoms to from CO_2. Above 200 K CO_2 immediately leaves the surface, due to its weak bonding to the surface. In contrast to the RuO_2(110) surface, the RuO_2(100) surface exposes also a catalytically inactive c(2×2) surface on which CO is not able to adsorb above 100 K. This inactive RuO_2(100)-c(2×2) phase may play an important role in the deactivation of RuO_2 catalysts in the electrochemical Cl_2 evolution[44] and other heterogeneous reactions.

At higher sample temperatures (say above 500 K) the mildly reduced RuO_2 surface transforms into a surface with small holes. For this restructuring process of the reduced RuO_2 surface a plausible mechanism is presented: Threefold coordinated O atoms from the surface are used to cap the 2f-cus Ru atoms, creating 3 Å deep holes in the surface. Excess Ru atoms agglomerate into small islands at the rims of such holes. In this way the RuO_2 surface becomes again stoichiometric, but covered with small Ru islands. Repeating CO reduction and annealing cycles lead to a rough surface that is finally completely covered by a metallic Ru film. The RuO_2 film is buried under the Ru film.[12]

We should emphasize that the (110), (101) and (100) orientations of RuO_2 are already active through their regular undercoordinated surface sites.[23, 55] Quite in contrast, the activity of typical oxide surface, such as TiO_2 and SnO_2, is determined by defects on the surface.[5]

7. Outlook

The ultimate goal of surface science is the atomic-scale design of catalysts with properties in activity and selectivity that are superior to conventional catalysts. To achieve this goal we have to find ways to modify purposely the active sites on the catalyst's surface and to engineer surface-mediated reaction pathways on a molecular level.

The (100) and (110) orientations of RuO_2(110) provide convenient systems for site-sensitive surface chemistry experiments, as the separation varies between the active site, that is, the undercoordinated oxygen atoms and the undercoordinated Ru atoms. For instance, the separation of active sites may exert strong influence on the dehydrogenation reaction of alcohols. The adsorption of the intact hydrocarbon molecule proceeds via the undercoordinated Ru atoms, while the abstracted H atoms are adsorbed over the bridging O atoms. The proper orientation may improve considerably the selectivity of the RuO_2 catalyst to a particular dehydrogenation reaction. Of course, we have to find experimental means to stabilize one orientation of RuO_2 over other possible orientations.

In recent publications, supported RuO_2 has demonstrated to be a promising and selective catalyst for the aerobic oxidation of alcohols to their corresponding aldehydes and ketones.[58, 59] Therefore, we are extending our STM studies to the partial oxidation of methanol to formaldehyde.[55] This reaction is much more complex than the oxidation of CO since the activation of O—H, C—H and C—O bonds are involved. Preliminary STM measurements differentiate at least between three intermediate species on the surface. Fourier transform IR spectroscopy (FTIR) as well as high resolution core level spectroscopy (HRCLS) measurements will be applied to identify the chemical nature of these surface intermediates.

Acknowledgements

We thank the LRZ in Munich for providing massive parallel computing time at the Hitachi supercomputer. The STM work in Vienna was supported by the "Fonds zur Förderung der wissenschaftlichen Forschung". The DFG is acknowledged for partial financial support (Ov21-4). Financial support by the Swedish Research Council is acknowledged by E.L.

Keywords: catalytic activity · oxide surfaces · ruthenium dioxide · scanning probe microscopy · surface chemistry

[1] J.M Thomas, W.J. Thomas, *Principles and Practice of Heterogeneous Catalysis*, VCH, **1996**.
[2] *Handbook of Heterogeneous Catalysis, Vol. 5* (Eds.: G. Ertl, H. Knözinger, J. Weitkamp), Wiley: New York, **1997**.
[3] See for example, various articles in *Surf. Sci.* **2001**, *500*, special issue.
[4] a) F. Besenbacher, I. Chorkendorff, B.S. Clausen, B. Hammer, A.M. Molenbroek, J.K. Nørskov, and I. Steensgaard, *Science* **1998**, *279*, 1913; b) C.J.H. Jacobsen, S. Dahl, B.S. Clausen, S. Bahn, A. Logadottir, J.N. Nørskov, *J. Am. Chem. Soc.* **2001**, *123*, 8404.
[5] V.E. Henrich, P.A. Cox, *The Surface Science of Metal Oxides*, Cambridge University Press, Cambridge, **1994**.
[6] C. Noguera, *Physics and Chemistry of Oxide Surface*, Cambridge University Press, Cambridge, **1996**.
[7] C.T. Champbell, *Surf. Sci.* **1997**, *27*, 1.
[8] M. Bäumer, H.-J. Freund, *Prog. Surf. Sci.* **1999**, *61*, 127.
[9] S.A. Chambers, *Surf. Sci. Rep.* **2000**, *39*, 105.
[10] W. Weiss, *Prog. Surf. Sci.* **2002**, *70*, 1.
[11] U. Diebold, *Surf. Sci. Rep.* **2003**, *48*, 53.
[12] H. Over, A.P. Seitsonen, E. Lundgren, M. Schmid, P. Varga; *Surf. Sci.* **2002**, *515*, 143.
[13] H. Over, A.P. Seitsonen, E. Lundgren, M. Schmid, P. Varga, *J. Am. Chem. Soc.* **2001**, *123*, 11807.

[14] H. Over, *Appl. Phys. A* **2002**, 75, 37.
[15] H. Over, M. Muhler, *Prog. Surf. Sci.* **2003**, 72, 3.
[16] A. P. Seitsonen, H. Over in *High Performance Computing in Science and Engineering in Munich 2002*, Springer-Verlag, **2003**, p. 171.
[17] H. Over, A. P. Seitsonen, *Science* **2002**, *297*, 2003.
[18] K. Thürmer, E. Williams, J. Reutt-Robbey, *Science* **2002**, *297*, 2033.
[19] Y. D. Kim, A. P. Seitsonen, H. Over, *Surf. Sci.* **2000**, *445*, 1.
[20] U. Diebold, J. E. Anderson, K.-O. Ng, D. Vanderbilt, *Phys. Rev. Lett.* **1996**, *77*, 1322.
[21] Y. D. Kim, S. Schwegmann, A. P. Seitsonen, H. Over, *J. Phys. Chem. B* **2001**, *105*, 2205.
[22] K. Kern, H. Niehus, A. Schatz, P. Zeppenfeld, J. George, and G. Comsa, *Phys. Rev. Lett.* **1991**, *67*, 855.
[23] Y. D. Kim, H. Over, G. Krabbes, G. Ertl, *Top. Catal.* **2001**, *14*, 95.
[24] A. P. Seitsonen, unpublished DFT calculations.
[25] Y. D. Kim, M. Knapp, H. Over, unpublished LEED results.
[26] W. F. Lin, M. S. Zei, Y. D. Kim, H. Over, G. Ertl, *J. Phys. Chem.* **2000**, *104*, 6040.
[27] Y. D. Kim, A. P. Seitsonen, S. Wendt, J. Wang, C. Y. Fan, K. Jacobi, H. Over, G. Ertl, *J.Phys. Chem. B* **2001**, *105*, 3752.
[28] A. Böttcher, H. Niehus, *Phys. Rev. B* **1999**, *60*, 14396.
[29] K. Reuter, M. Scheffler, *Phys. Rev. B* **2002**, *65*, 035406.
[30] S. Wendt, M. Knapp, H. Over, *J. Am. Chem. Soc.*, in press.
[31] The first isotope labeling experiments were performed by A. Böttcher, H. Conrad, H. Niehus, *Surf. Sci.* **2001**, *478*, 221. However, the interpretation of the exchange of adsorbed O atoms into the subsurface region is untenable. A correct interpretation of these results in terms of exchange of on-top and bridging O atoms was first given by Wendt et al.[30]
[32] A. Böttcher, M. Rogozia, H. Niehus, H. Over, G. Ertl, *J. Phys. Chem. B* **1999**, *103*, 6267.
[33] C. Y. Fan, J. Wang, K. Jacobi, G. Ertl, *J. Phys. Chem.* **2001**, *114*, 10058.
[34] Z.-P. Liu, P. Hu, A. Alavi, *J. Chem. Phys.* **2001**, *114*, 5957.
[35] S. Wendt, A. P. Seitsonen, Y. D. Kim, M. Knapp, H. Idriss, H. Over, *Surf. Sci.* **2002**, *505*, 137.
[36] Y. D. Kim, A. P. Seitsonen, H. Over, *Phys. Rev. B* **2001**, *63*, 115419.
[37] A. P. Seitsonen: www.iki.fi/~apsi/Science/movies/
[38] A. P. Seitsonen, Y. D. Kim, M. Knapp, S. Wendt, H. Over, *Phys. Rev. B* **2002**, *65*, 05413.
[39] H. Over, Y. D. Kim, A. P. Seitsonen, S. Wendt, E. Lundgren, M. Schmid, P. Varga, A. Morgante, G. Ertl, *Science* **2000**, *287*, 1474.
[40] a) N. Bronsted, *Chem. Rev.* **1928**, *5*, 231; b) M. G. Evans, N. P. Polanyi, Trans. *Faraday Soc.* **1936**, *32*, 1333.
[41] J. N. Norskov, T. Bligaard, A. Logadottir, S. Bahn, L. B. Hansen, M. Bollinger, H. Bengaard, B. Hammer, Z. Slijvancanin, M. Mavrikakis, Y. Xu, S. Dahl, C. J. H. Jacobsen, *J. Catal.* **2002**, *209*, 275.
[42] A. Michaelides, Z. P. Liu, C. J. Zhang, A. Alavi, D. A. King, P. Hu, *J. Am. Chem. Soc.* **2003**, *125*, 3704.
[43] M. Knapp, A. P. Seitsonen, H. Over, unpublished results.
[44] R. Mason, A. Mills, D. Milton, *J. Less-Common Met.* **1989**, *155*, 89, and references therein.
[45] U. Diebold, J. Lehman, T. Mahmoud, M. Kuhn, G. Leonardelli, W. Hebenstreit, M. Schmid, P. Varga, *Surf. Sci.* **1998**, *411*, 137.
[46] R. Schaub, E. Wahlström, A. Ronnau, E. Lagsgaard, I. Steensgaard, F. Besenbacher, *Science* **2003**, *299*, 377.
[47] M. Li, W. Hebenstreit, U. Diebold, A. M. Tyryshkin, M. K. Bowman, G. G. Dunham, M. A. Henderson, *J. Phys. Chem.* **2000**, *104*, 4944.
[48] a) H. Onishi, Y. Iwasawa, *Surf. Sci.* **1994**, *313*, L783; b) R. A. Bennet, S. Poulston, P. Stone, M. Bowker, *Phys. Rev. B* **1999**, *59*, 10341; c) A. Berko, F. Solymosi, *Langmuir* **1996**, *12*, 1257; d) P. W. Murray, N. G. Condon, N. G. Thornton, *Phys. Rev. B* **1995**, *51*, 10989; e) M. Sander, T. Engel, *Surf. Sci.* **1995**, *329*, 241; f) R. E. Tanner, M. R. Castell, G. A. D. Briggs, *Surf. Sci.* **1998**, *412/413*, 672; g) C. Xu, X. Lai, G. W. Zajac, D. W. Goodman, *Phys. Rev. B* **1996**, *56*, 13464; h) D. Novak, E. Garfunkel, T. Gustafsson, *Phys. Rev. B* **1994**, *50*, 5000.
[49] N. M. Harrison, X. G. Wang, J. Muscat, M. Scheffler, *Faraday Discuss. Chem. Soc.* **1999**, *114*, 305.
[50] G. Charlton, P. B. Hoowes, C. L. Nicklin, P. Steadman, J. S. G. Taylor, C. A. Muryn, S. P. Harte, J. Mercer, R. McGrath, D. Norman, T. S. Turner, G. Thornton, *Phys. Rev. Lett.* **1997**, *78*, 495.
[51] H. Zajonz, H. L. Meyerheim, T. Gloege, W. Moritz, D. Wolf, *Surf. Sci.* **1998**, *398*, 369.
[52] E. Landree, L. D. Marks, P. Zschack, C. J. Gilmore, *Surf. Sci.* **1998**, *408*, 300.
[53] M. Li, W. Hebenstreit, U. Diebold, *Surf. Sci.* **1998**, *414*, L951.
[54] H. Idriss, M. A. Barteau, *Adv. Catal.* **2000**, *45*, 261.
[55] H. Madhavaram, H. Idriss, S. Wendt, Y. D. Kim, M. Knapp, H. Over, J. Aßmann, E. Löffler, M. Muhler, *J. Catal.* **2001**, *202*, 296.
[56] L. Zang, H. Kisch, *Angew. Chem.* **2000**, *112*, 4075; *Angew. Chem. Int. Ed.* **2000**, *39*, 3921.
[57] J. Aßmann, E. Löffler, A. Birkner, M. Muhler, *Catal. Today* **2003**, *85*, 235.
[58] K. Yamaguchi, N. Mizuno, *Angew. Chem.* **2002**, *114*, 4720; *Angew. Chem. Int. Ed. Engl.*, **2002**, *41*, 4538.
[59] B.-Z. Zhan, M. A. White, T.-K. Sham, J. A. Pincock, R. J. Doucet, K. V. R. Rao, K. N. Robertson, T. S. Cameron, *J. Am. Chem. Soc.* **2003**, *125*, 2195.

Received: May 9, 2003 [M833]
Revised: August 21, 2003

